Analysis of the Mechanical Properties of SMAW welded Joints on API 5LX42 Steel Pipelines

Abdelhamid Benhamel
Ecole Superieure en Sciences Appliquees de Tlemcen, BP 165 RP Bel Horizon, 13000 Tlemcen, Algeria
benhamel.abdelhamid@gmail.com(corresponding author)

Fethi Hadjoui
Department of Mechanical Engineering, University of Tlemcen 13000, Algeria
hadjoui_fethi@yahoo.fr

Abdelhamid Hadjoui
Department of Mechanical Engineering, University of Tlemcen 13000, Algeria
hadjoui_ab@yahoo.fr

Received: 4 November 2024 | Revised: 22 December 2024 | Accepted: 7 January 2025

 DOI: https://doi.org/10.48084/etasr.9495

ABSTRACT

This paper examines the performance of gas pipeline welding in relation to the mechanical properties and metallurgical structure of the weld bead. Our research focuses on API 5L X42 steel pipes, which are commonly used for transporting hydrocarbons, particularly in the welded joints of these pipes. We conducted tests to characterize a weld created using the Shielded Metal Arc Welding (SMAW) method for gas pipelines. This included a microstructural analysis of the heterogeneous zone and the production of standardized specimens taken perpendicular to the welding direction, which were then subjected to uniaxial tension to assess the properties of both the base material and the filler metal under various stress conditions. Our findings indicate that the welded joint exhibits hardening compared to the base metal due to thermal effects, and we observed that the elongation in the welded specimens is significantly lower than that of the unwelded specimens.

Keywords-API X42 steel; shielded metal arc welding; fatigue

I. INTRODUCTION

Pipelines play a very important role in industry and in particular in oil transport or production conditions which require the use of very high pressures, therefore the most effective method for joining high-strength steel (HSLA) pipes is welding [1-11]. In order to avoid bursting and damage to welded pipes due to geometry defects, corrosion and many intrinsic factors (inclusions, lack of penetration, gas pore), etc. [2-4], we are always looking for better mechanical properties of weld joints. The oil industry attaches great importance to the quality of pipe welding. This type of assembly is particularly distinguished by areas of heterogeneity, which reflect very different microstructures and mechanical characteristics, so it is necessary to identify them in order to consider them during the installation of the gas pipeline network [5].

In this paper, we first present the chemical compositions of the materials used and the main parameters of the welding process applied in a pipeline in service. Then, we treat the mechanical characteristics by destructive tests [6] and before concluding, we present the results obtained with interpretation. The aim of this work is twofold: to conduct experimental tests to evaluate the tensile strength of the weld joints and develop numerical models to predict the strength of the welded joints under external loads.

II. EXPERIMENTAL STUDY

The pipeline steel that we considered in our study is an API 5L X42 grade manganese micro-alloyed steel.

A. Material Characteristics

1) Base Metal

The chemical composition and the mechanical characteristics are indicated in Tables I and II.

2) Filler Metal

E6010 and E7010 are types of cellulose-Na electrodes specifically designed for DC welding. They offer a deep

penetration arc, are easy to use, and provide high efficiency and excellent detachment during welding. These electrodes are suitable for all welding positions. It is possible for the weld to form on both sides,with the chemical composition and mechanical properties detailed in Tables III-IV.

TABLE I. CHEMICAL ANALYSIS (%) OF API L X42 GRADE STEEL

C	Mn	Si	P	S	Cr	Mo
0.18	1.10	0.25	0.019	0.014	0.050	0E.025
V	**Al**	**Cu**	**Sn**	**Ni**	**Ti**	
0.040	0.040	0.060	0.035	0.030	0.039	

TABLE II. MECHANICAL PROPERTIES OF API L X42 GRADE STEEL

Type	Young's modulus (MPa)	Poisson's ratio	Yield strength (MPa)
API 5L X42	210	0.3	450

TABLE III. CHEMICAL ANALYSIS OF E6010 ANDE7010 FILLER METAL

	C	Mn	Si	P
E6010	≤ 0.2	0.3 - 0.6	≤ 0.02	≤ 0.04
E7010	0.2	0.6	0.6	0.09
	S	**Cr**	**Mo**	**V**
E6010	≤ 0.035	0.2	0.3	0.8
E7010	0.09	0.3	0.5	0.1

TABLE IV. MECHANICAL PROPERTIES OF E6010 ANDE7010 FILLER METAL

	Type	Young's modulus (MPa)	Rm (MPa)	Poison's ratio
Filler metal	E6010	128	≥ 420	0.34
	E7010		≤ 0.02	0.34
	Type	**Yield strength (MPa)**	**A (%)**	
Filler metal	E6010	330	27	
	E7010	500	26	

B. Welding Process

The assembly is done with the coated electrode.

1) Preparation

The edges to be welded were firstly prepared. They were freed of any excess oxides, rust, grease, or paint. The passes are only schematic and the exact arrangements of the passes depend on the chosen welding parameters.

2) Fixing

Fixing was conducted by external or internal clamps to avoid deformations. The internal fastener was removed after 100% completion of the first pass. The technique of execution of the welded joint and the electrical characteristics are shown in Table V.

3) Machining of the Specimen

To analyze the weld regions, specimens were machined from a section of pipe featuring a butt weld joint, made from API 5L X42 steel with E6010 as filler material. It is essential that these specimens do not undergo deformation during the machining process, which could result from the relaxation of residual stress. All test specimens should be sourced from the same welded pipe. The machining was conducted under standard ambient conditions while adhering to specific machining parameters. The machining speed was adjusted according to the specimen's geometry, resulting in a different speed than what would typically be used in actual machining scenarios. Figures 1-3 illustrate the pipe-cutting machine, the visual appearance of the weld bead, and the universal milling machine WEYRAUCH FR-U-1100.

TABLE V. ELECTRICAL PROPERTIES OF THE WELDING PROCESS

Passes	1st pass	2nd pass	3rd pass	4rd pass
Welding process	SMAW	SMAW	SMAW	SMAW
Welding position	5G ↗	5G ↙	5G ↙	5G ↙
Fixed rotation	Fixed	Fixed	Fixed	Fixed
Current/Polarity	DC-EN	DC-EP	DC-EP	DC-EP
Filler metal	E6010	E7010	E7010	E7010
Electrode diameter (mm)	3.25	3.25	4	4
Amperage	80-135	90-140	110-150	110-150
Tension	30-35	25-35	30-40	30-40

Fig. 1. Cutting a section of the welded pipe.

Fig. 2. Visualization of the shape of the welded joint.

4) Tensile Tests

The tensile tests were carried out in the mechanical test laboratory on a universal machine of the Zwike/role type with a capacity of 120 tons under ambient temperature.

Fig. 3. Universal milling machine WEYRAUCH FR-U-1100.

5) Fatigue Tests

Fatigue testing machines cover a variety of fatigue applications, dynamic and static testing are based on servo-hydraulic and eclectic motor technologies. These fatigue tests were carried out on the INSTRON 8502 type testing machine under the following conditions: Machine capacity: 10 tonnes, +62 undulating sinusoidal tensile stress, load ratio R=0.1, frequency f=30 Hz, and ambient temperature. The purpose of these tests was to study the mechanical behavior of the materials of the pipeline with and without welding in an ambient medium by tensile curves in order to draw the Wöhler curves. The results will consider thousands of cycles, which determine the life of the welded joints.

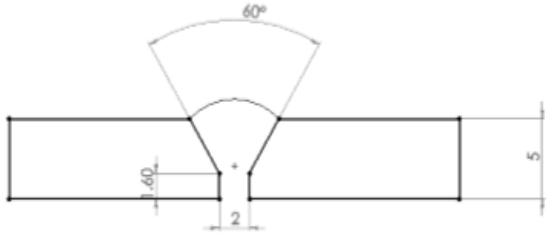

Fig. 4. Welded joint geometry.

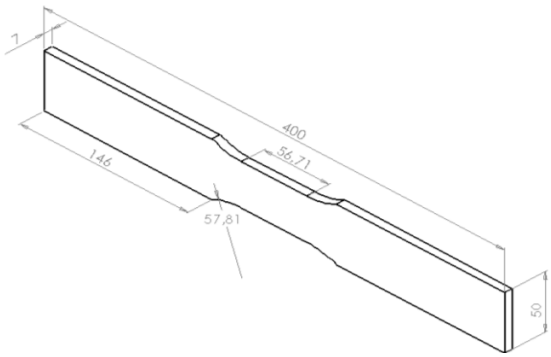

Fig. 5. Test specimen of steel API 5L X42 (not welded) for tensile strength testing.

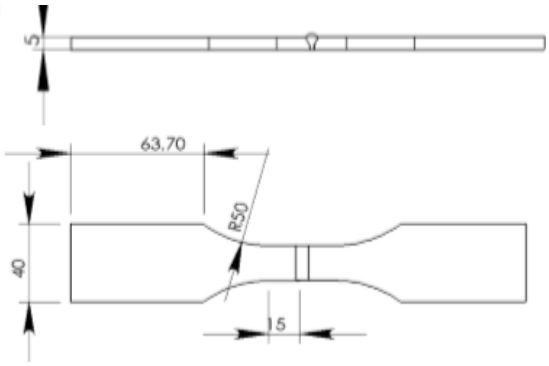

Fig. 6. Test specimen with welded joint for traction in API 5L X42 steel (with weld beads).

III. FINITE ELEMENT SIMULATION

We used numerical simulations through the finite element method, which allows us to understand the behavior of the weld and predict its life span. Finite element simulation allows us to predict the resistance to forces acting on welded joints. Very often, material test data are provided using nominal stress values. In such situations, the expressions presented below must be used to convert the plastic material data from nominal stress/strain values to true stress tress/strain values. The relationship: between true stress/strain and nominal stress /strain are [12, 14]:

$$\sigma_{nominal} = \frac{F[N]}{S[m^2]} \quad (1)$$

$$\varepsilon_{nom} = \frac{\Delta L}{L_0} \quad (2)$$

$$\sigma_{true} = \sigma_{nom} \times (1 + \varepsilon_{nom}) \quad (3)$$

$$\varepsilon_{true} = ln(1 + \varepsilon_{nom}) \quad (4)$$

$$\varepsilon_{plastique} = \varepsilon_{true} - \frac{\sigma_{true}}{E} \quad (5)$$

where ε is the strain, σ is the stress, F is the applied force (N), and S represents the section (m^2). Subscripts *nom* and *true* stand for nominal and true values, respectively.

IV. RESULTS AND DISCUSSION

The mechanical characteristics of the material studied (API X42 steel) are illustrated in the following figures. The results reported in Tables VI and VII express the average values of the tests. It should be noted that the obtained results comply with the mechanical characteristics provided by the manufacturer.

TABLE VI. MECHANICAL CHARACTERISTICS OBTAINED BY TENSILE TEST

Young's modulus (MPa)	Elastic limit (MPa)	Constraints max (MPa)	Elongation (%)
210000	460	510	54

The static and cyclic mechanical characteristics of the welded structure are summarized in Figure 8. We notice cyclic hardening of the material compared to the static case, which gives us an explanation why fatigue is the cause of the failure of welded structures.

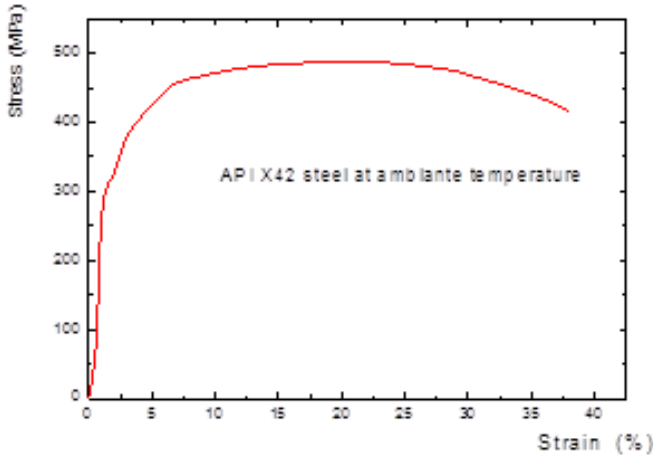

Fig. 7. Tensile curve of an API 5L X42 steel test specimen.

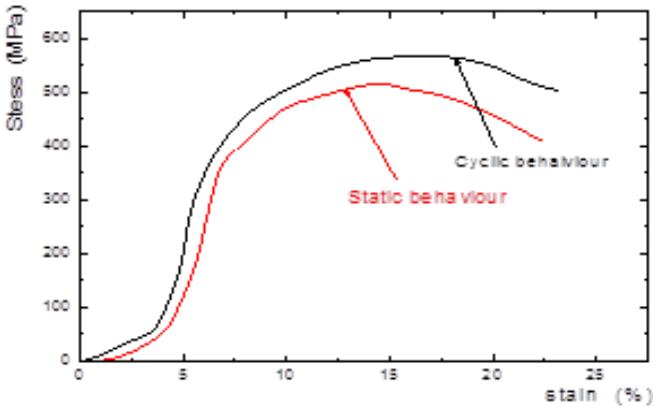

Fig. 8. Static and cyclic behavior of the welded structure.

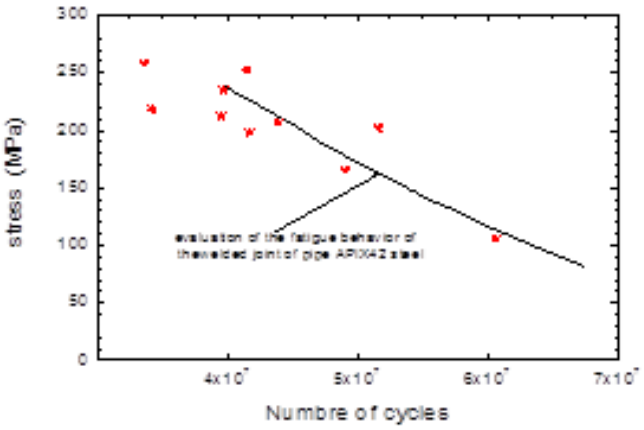

Fig. 9. Wöhler curve of the welded pipeline in fatigue.

According to Figure 10 and Table VII, there is a hardening in the weld joint compared to the base metal due to the thermal effect of welding and the elongation is less important than that of the seamless specimen.

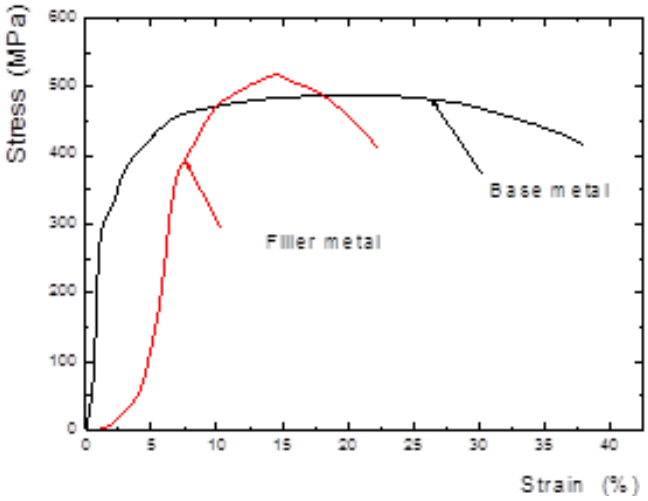

Fig. 10. Behavior of base metal and filler metal by tensile test.

TABLE VII. MECHANICAL CHARACTERISTICS OF THE SPECIMEN WITH WELDED JOINT AFTER TENSILE TEST

Elastic limit (MPa)	Constraints max (MPa)	Elongation (%)
450	550	23

Using Abaqus finite element simulation software, a 3D numerical model was developed to replicate the transverse tensile test of welded specimens (Figure 11). The material was assumed to exhibit elastic-plastic behavior. The model was treated as a deformable body, incorporating an elasticity criterion along with suitable stress-strain relationships during nonlinear plasticity. For the elastic analysis, the material's elastic properties were characterized by the modulus of elasticity (E) and poison ratio (υ).The finite element discretization employed 3D 8-node isoparametric hexahedral elements. For simplicity, the sample was positioned in the Oxy plane, and the tensile test was simulated by applying positive displacement in the Ox direction. Figure 12 shows the comparison of the numerical and experimental results.

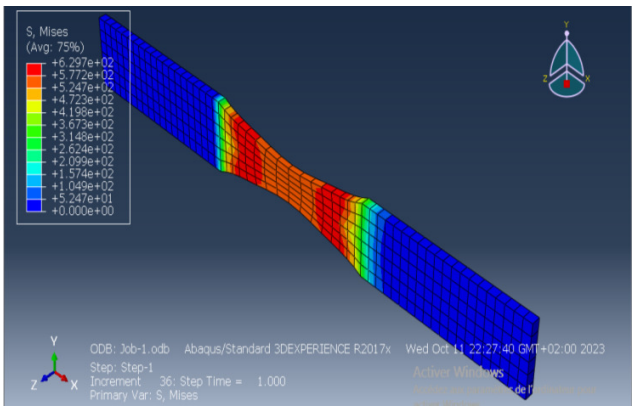

Fig. 11. Distribution of the Von Mises stresses of the API 5 L X42 steel specimen in tension.

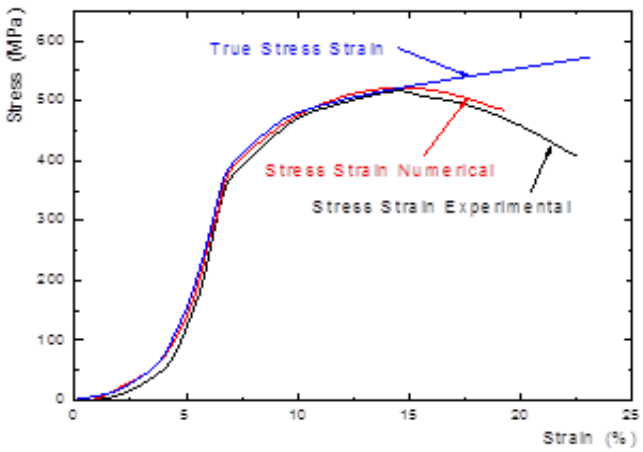

Fig. 12. Comparison between numerical and experimental curve.

V. CONCLUSION

In this study, we presented a method that involves understanding the welding process using the SMAW technique. We conducted tests using operating parameters applied to accurately target the encountered issues. The analysis of samples with and without welding allowed us to highlight the significance of the results obtained on the welded samples, where welding alters their mechanical properties and enhances fatigue resistance under cyclic loading. Furthermore, numerical simulation using finite element analysis with Abaqus software allowed us to clearly illustrate the experimental phenomena.

Welded joints exhibit mechanical characteristics different from those of the base metal, with an increase in hardness but a decrease in elongation compared to the non-welded samples due to the thermal effect. The use of digital tools allows us to predict the behavior of welded joints by varying the welding parameters, in this case, the number of passes, the thickness of tubes and the materials used.

These new areas, which will modify the elasticity and metallurgy of the structure, will require a relaxation heat treatment protocol to improve their mechanical behaviour.

REFERENCES

[1] A. Mebrek and M. Mokhtari, "Analyse experimentale des caracteristiques mecaniques obtenues dans le sens parallele et perpendiculaire du laminage des pipelines, gradeX42," in *3rd International Conference on welding, nondestructive testing and the industry of materials and alloys (ICWNDT-MI'12)*, Oran, Algeria, Nov. 2012.

[2] M. Holicky, J. Markova, M. Sykora, "Target Reliability Levels in Present Standards," *Transactions of the VŠB – Technical University of Ostrava*, vol. 14, no. 2, 2014, Art. no. 18.

[3] E. Kormanikova and K. Kotrasova, "Sizing optimization of sandwich plate with laminate faces," *International Journal of Mathematics and Computers in Simulation*, vol. 10, pp. 273–280, 2016.

[4] J. Vican, J. Gocal, J. Odrobinak, M. Moravcik, and P. Kotes, "Determination of Railway Bridges Loading Capacity," *Procedia Engineering*, vol. 111, pp. 839–844, Jan. 2015, https://doi.org/10.1016/j.proeng.2015.07.155.

[5] J. M. Melenk and I. Babuška, "The partition of unity finite element method: Basic theory and applications," *Computer Methods in Applied Mechanics and Engineering*, vol. 139, no. 1, pp. 289–314, Dec. 1996, https://doi.org/10.1016/S0045-7825(96)01087-0.

[6] O. C. Zienkiewicz, J. P. De S.R. Gago, and D. W. Kelly, "The hierarchical concept in finite element analysis," *Computers & Structures*, vol. 16, no. 1, pp. 53–65, Jan. 1983, https://doi.org/10.1016/0045-7949(83)90147-5.

[7] M. Krejsa, J. Brozovsky, D. Mikolasek, P. Parenica, L. Koubova, and A. Materna, "Numerical Modeling of Fillet and Butt Welds in Steel Structural Elements with Verification Using Experiment," *Procedia Engineering*, vol. 190, pp. 318–325, Jan. 2017, https://doi.org/10.1016/j.proeng.2017.05.344.

[8] X. L. Chen, Z. Yang, and F. W. Brust, "Modeling distortion and residual stress during welding: practical applications," in *Processes and Mechanisms of Welding Residual Stress and Distortion*, Z. Feng, Ed. Sawston, UK: Woodhead Publishing, 2005, pp. 225–263.

[9] K. Abdullah, P. M. Wild, J. J. Jeswiet, and A. Ghasempoor, "Tensile testing for weld deformation properties in similar gage tailor welded blanks using the rule of mixtures," *Journal of Materials Processing Technology*, vol. 112, no. 1, pp. 91–97, May 2001, https://doi.org/10.1016/S0924-0136(01)00555-6.

[10] M. Allouti, "Study of the harmfulness of defects in pipelines such as scratches, dents or their combinaisons," Ph.D. dissertation, Paul Verlaine University - Metz, Metz, France, 2010.

[11] D. G. Zisopol, M. Minescu, and D. V. Iacob, "A Study on the Influence of aging of the Butt-welded PE100 SDR11 on Shore A Hardness and Tensile Strength," *Engineering, Technology & Applied Science Research*, vol. 14, no. 1, pp. 12722–12727, Feb. 2024, https://doi.org/10.48084/etasr.6635.

[12] P. Quang and T. Toan, "Simulation and Experimental Test in Tensile Behaviour of Austenitic Stainless Steels," *Advances in Materials*, vol. 8, no. 3, pp. 108–111, Jul. 2019, https://doi.org/10.11648/j.am.20190803.12.

[13] P. Dai, Y. Wang, S. Li, S. Lu, G. Feng, and D. Deng, "FEM analysis of residual stress induced by repair welding in SUS304 stainless steel pipe butt-welded joint," *Journal of Manufacturing Processes*, vol. 58, pp. 975–983, Oct. 2020, https://doi.org/10.1016/j.jmapro.2020.09.006.

[14] I. Scheider, W. Brocks, and A. Cornec, "Procedure for the Determination of True Stress-Strain Curves From Tensile Tests With Rectangular Cross-Section Specimens," *Journal of Engineering Materials and Technology*, vol. 126, no. 1, pp. 70–76, Jan. 2004, https://doi.org/10.1115/1.1633573.

[15] H. D. Kweon, J. W. Kim, O. Song, and D. Oh, "Determination of true stress-strain curve of type 304 and 316 stainless steels using a typical tensile test and finite element analysis," *Nuclear Engineering and Technology*, vol. 53, no. 2, pp. 647–656, Feb. 2021, https://doi.org/10.1016/j.net.2020.07.014.